

Highly permselective MIL-68(Al)/matrimid mixed matrix membranes for CO₂/CH₄ separation

Xinyu Dong,^{1,2} Qian Liu,¹ Aisheng Huang¹

¹Institute of New Energy Technology, Ningbo Institute of Material Technology and Engineering, CAS, 1219 Zhongguan Road, Ningbo 315201, People's Republic of China

²Key Laboratory for Microstructures, Shanghai University, Shanghai 200444, People's Republic of China

Correspondence to: A. Huang (E-mail: huangaisheng@nimte.ac.cn)

ABSTRACT: With global appeal to green and efficient utilization of energies, metal-organic frameworks based mixed matrix membranes are standing out in applications such as gas and liquid separation because of the integration of size/shape selectivity of MOFs with processability and mechanical stability of polymers. In the present work, a novel MIL-68(Al) (MIL = Material of Institute Lavoisier) based mixed matrix membrane (MMM) was developed by adding porous MIL-68(Al) into Matrimid for the separation of CO₂/CH₄ mixture. The MIL-68(Al)/Matrimid MMM displays a high CO₂ permselectivity. For the separation of an equimolar CO₂/CH₄ mixture at 373 K and 1 bar, the CO₂ permeability and the CO₂/CH₄ selectivity are 284.3 Barrer and 79.0, respectively, which far exceed the Robeson upper bound limit and those of the previously reported MMMs. Both the operation pressure and temperature have great influence to the separation performance of the MIL-68(Al)/Matrimid MMM. Further, the MIL-68(Al)/Matrimid MMM shows a high stability in the long-term separation of CO₂/CH₄. These properties recommend the MIL-68(Al)/Matrimid MMM as a promising candidate for the purification of natural gases. © 2016 Wiley Periodicals, Inc. *J. Appl. Polym. Sci.* **2016**, *133*, 43485.

KEYWORDS: composites; membranes; porous materials; polyimides; separation techniques

INTRODUCTION

Natural gas has long been exploited as the source of energy for both domestic and industrial applications because of its high energy efficiency and eco-compatibility. However, most raw natural gases contain undesirable impurity CO₂ with concentration as high as 70%.¹ The presence of CO₂ will reduce the energy efficiency of natural gases, and corrode pipelines in the presence of water.^{1–4} Consequently, effective separation techniques are highly desired to separate CO₂ from natural gases. Conventional technologies like pressure swing adsorption (PSA) and cryogenic distillation are energy-intensive, operation-complex, and environment-hurting. Therefore, a clean and energy-economical separation technique is desired.

Membrane-based separation has been considered to be the most promising alternative because of its low energy consumption, ease of operation, and cost effectiveness.^{5–7} The polymeric membranes have dominated industrial applications because of their low cost and easy preparation. However, the performances of traditional polymeric membranes are limited by a trade-off between permeability and separation selectivity.^{8,9} Furthermore, polymeric membranes are easy to plasticize by some gases or

vapors like CO₂ or H₂O, resulting in severe reduction in their separation performances.¹⁰ To solve these problems, various strategies have been developed, including modification of polymer structure, blending of different polymers, and fabrication of mixed matrix membranes (MMMs).^{11–15} MMMs are a type of hybrid membranes characterized by the incorporation of inorganic fillers into polymer matrix, making use of both easy processability of the polymer and flexibility of the filler to enhance the permselective performance of membranes.^{16–18} Various inorganic porous materials such as zeolites, silica, carbon nanotubes, and newly emerged MOFs, were incorporated into polymer matrices to enhance the performances of polymeric membranes.^{19–25} MOFs are a fascinating kind of porous materials built with metal ions and organic linkers. Because of their excellent thermal stability, favorable pore regularity, and high surface area, MOFs have attracted intense attention in potential applications such as gas storage and adsorption, gas separation, catalysis, and drug delivery.^{26–33} Because the organic linkers in MOFs have excellent affinity with polymer chains, MOF-based MMMs display outstanding separation performances.^{34–37} Generally, MMMs with both high permeability and high separation selectivity are desirable in practical applications. To achieve

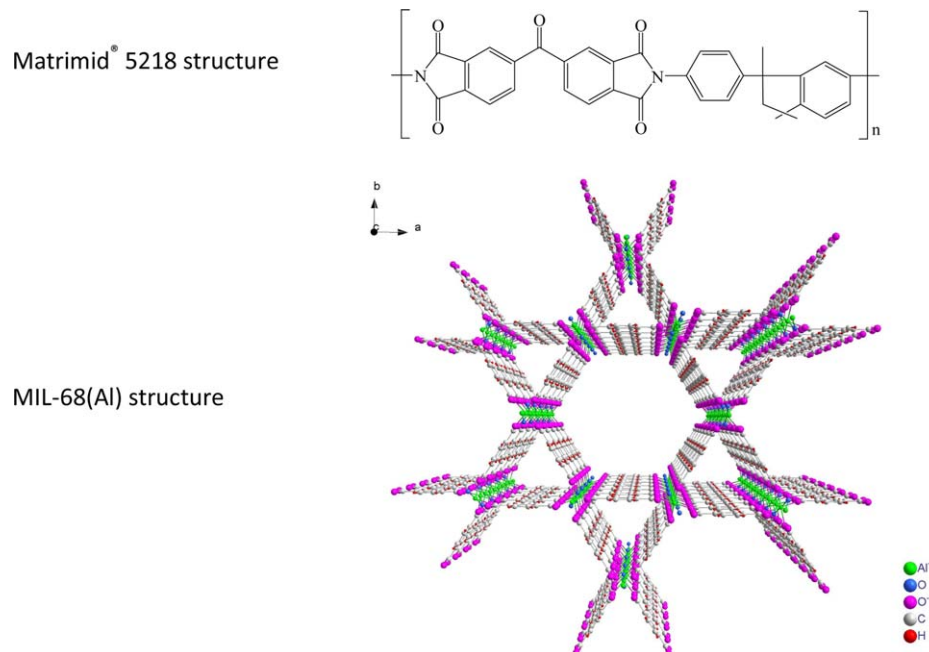


Figure 1. Chemical structure of Matrimid 5218 and the MIL-68(Al) crystal structure viewed along [001] direction. [Color figure can be viewed in the online issue, which is available at wileyonlinelibrary.com.]

these aims, a rational choice of matrix/filler pair plays an important role in successful preparation of MMMs.^{38,39} Moreover, in practical usage, the operation conditions, especially operation pressure and temperature, are of great importance.^{40,41} Guo *et al.* probed into the influence of pressure on the CO₂/CH₄ separation performances of NH₂-MIL-125(Ti)/PSF MMMs and found that both the CO₂ permeability and CO₂/CH₄ separation factor decreased with increasing pressure.⁴²

MIL-68(Al) is a MOF of the MIL category. It has infinite chains of corner-sharing metal-centered octahedral AlO₄(OH)₂ linked via hydroxyl groups and terephthalate ligands (Figure 1). There are two kinds of channels with opening diameters of 6.0–6.4 Å and 16–17 Å for its triangular and hexagonal pores, respectively.⁴³ It is expected that such a one-dimensional large-pore structure can facilitate the diffusion of gases, thus significantly increasing the gas permeability. Furthermore, MIL-68(Al), with a large surface area of 1417 m²·g⁻¹ (pore volume 0.67 cm³·g⁻¹ and particle density 0.84 g·cm⁻³), has plentiful hydroxyl groups along the channel directions, showing strong adsorption affinity to CO₂ and potential selectivity of CO₂ over CH₄.^{27,43} It is well recognized that the CO₂-selective materials as fillers can simultaneously improve the permeability and selectivity of MMMs for CO₂ separation.^{42,44} An additional merit is that the MIL-68(Al) shows good chemical stability toward water, which is helpful for the practical utility under real industrial conditions, because water vapor exists inevitably in most natural gas wells.²⁷ Attributing to these merits, MIL-68(Al) is expected to be a promising candidate to prepare CO₂-selective MMMs for the separation of CO₂/CH₄. Recently, Seoane *et al.* reported the synthesis of MIL-68(Al)/Polysulfone MMMs for the separation of H₂/CH₄ and CO₂/CH₄.⁴⁵ However, the separation performances of the MIL-68(Al)/Polysulfone MMMs were limited by the poly-

sulfone polymer whose permselectivity is far below the Robeson upper bound, thus a better choice of filler/matrix pair is desired.

The glassy polymer Matrimid® 5218 (Figure 1) is widely selected as matrix because of its outstanding separation performance for CO₂/CH₄, whose permselectivity is close to the trade-off limit of the Robeson's plot.^{3,5,6,46} In this work, we incorporate MIL-68(Al) into Matrimid matrix to prepare MIL-68(Al)/Matrimid MMMs for CO₂/CH₄ separation. This combination of highly porous fillers and high performance matrix is expected to prepare membranes with high CO₂ permeability and selectivity over CH₄. To the best of our knowledge, this is the first report of MIL-68(Al)/Matrimid MMMs. The separation of CO₂/CH₄ by using the MIL-68(Al)/Matrimid MMMs is investigated in detail, focusing on the effect of operation pressure and temperature on the separation performances.

EXPERIMENTAL

Chemicals

All chemicals were used as received: terephthalic acid (Alfa Aesar, 99%), aluminum chloride hexahydrate (AlCl₃·6H₂O, Alfa Aesar, 99%), N, N'-dimethylformamide (DMF, Carlo Erba, pure), Matrimid® 5218 polyimide polymer (VWR International GmbH), methanol (Sinopharm, 99.5%), and chloroform (Sinopharm, 99%).

Synthesis of MIL-68(Al)

MIL-68(Al) was synthesized according to previously reported procedures.⁴³ In a typical synthesis, 5 g (30 mmol) terephthalic acid and 4.88 g (20 mmol) AlCl₃·6H₂O were dissolved in 284 g (3891 mmol) DMF. The mixture was placed in a round bottom flask equipped with condenser, continuously stirred, and heated at 403 K for 18.5 h in oil bath. After the mixture cooled down

naturally to room temperature, a yellow solid was separated by filtration. To eliminate the free acid remaining in the pores, the as-synthesized solid was washed with 50 mL DMF for three times, and subsequently washed with 50 mL methanol for four times at ambient temperature under continuous stirring, and then some light yellow solid was obtained.

Preparation of MIL-68(Al)/Matrimid MMMs

MIL-68(Al)/Matrimid MMMs were prepared by following the procedures described elsewhere with minor modification.³⁴ Before preparation of MIL-68(Al)/Matrimid MMMs, Matrimid, and MIL-68(Al) crystals were heated overnight at 393 K in a conventional oven to remove adsorbed water and residual solvent. Under the same fabrication condition, a filler loading of 10% was certified to be the optimal loading for MIL/Matrimid pair in previous literature.¹⁷ Therefore, the loading of 10% was employed for a further comprehensive evaluation of operation pressure and temperature. In a typical synthesis, 0.04 g MIL-68(Al) was added into 3.6 g chloroform, and then the mixture was treated with sonication for 15 min to get a well-dispersed solution. Thereafter, 0.36 g Matrimid was added into the solution, and the resulted solution was kept stirring for 48 h at room temperature to obtain a homogeneous solution for membrane preparation.

Flat-scraping method was used for membrane-casting. The homogeneous solution was poured onto a flat glass plate and was quickly scraped with a membrane fabricator. Within a few minutes, the membrane was dried and immediately peeled off from the glass plate, and annealed at 453 K for 16 h. The annealing step is important to remove residual solvent and activate filler crystals.^{34,43} The MIL-68(Al)/Matrimid MMMs generally have a thickness of 20 (± 2) μm , as measured with a digital micrometer (Guilin Guanglu Measuring Instrument).

Characterizations of MIL-68(Al) Crystals and MIL-68(Al)/Matrimid MMMs

The phase purity and crystallinity of the MIL-68(Al) crystals and MIL-68(Al)/Matrimid MMMs were characterized by X-ray diffraction (XRD). The XRD patterns were recorded at room temperature under ambient conditions with Bruker D8 ADVANCE X-ray diffractometer with CuKa radiation at 40 kV and 40 mA.

The morphology and crystal size of the MIL-68(Al) crystals, as well as the morphology and thickness of the MIL-68(Al)/Matrimid MMMs were characterized by field emission scanning electron microscopy (FESEM). FESEM micrographs were taken on an S-4800 (Hitachi) with a cold field emission gun operating at 4 kV and 10 μA . All membrane samples were made with freeze-fracture method and coated with platinum before characterization.

Single Gas Permeation and Mixture Gas Separation

The MIL-68(Al)/Matrimid MMMs were evaluated by single gas permeation and mixture gas separation in a Wicke-Kallenbach permeation apparatus.^{47,48} For gas permeation, the MIL-68(Al)/Matrimid MMMs were sealed in a permeation module with silicone O-rings and checked by leakage detection. Because of a very low permeability of CH₄ at room temperature, which was

almost undetected by gas chromatograph (GC, Echrom A90), the gas permeation and separation experiment was evaluated at a temperature higher than 373 K in all the cases. The sweep gas N₂ (50 mL min⁻¹) was fed on the permeate side to keep the concentration of the permeating gas as low as possible, thus providing a driving force for permeation. Single gases CO₂ (50 mL min⁻¹) and CH₄ (50 mL min⁻¹) as well as equimolar mixture CO₂/CH₄ (both 50 mL min⁻¹) were fed on the feed side of the permeation module. For both single gas permeation and mixture gas separation, the fluxes of feed and sweep gases were determined with mass flow controllers, and a calibrated GC was used to measure the gas concentrations.

For data collection and calculation, single gas permeability was calculated with the following equation³⁴:

$$P = \frac{VL}{A p_{feed} T_0} \left(\frac{dp}{dt} \right) \quad (1)$$

where P is the permeability of the permeated gas, generally expressed as Barrer (1 Barrer equals to 10^{-10} cm³ (STP) cm cm⁻² s⁻¹ cmHg⁻¹); V is the volume of permeation (cm³); l is the thickness of the membrane (cm); A is the effective area of the membrane (cm²); T is the absolute operating temperature (K); T_0 is the standard-state temperature (273.15 K); p_{feed} is the pressure of the feed gas (cmHg); p_0 is the standard-state pressure (76 cmHg); dp/dt is the increasing rate of pressure in the permeating volume at steady state (cmHg s⁻¹).

Ideal separation factor was calculated from the single gas permeabilities P_i and P_j as in the following equation⁴⁹:

$$\alpha_{ij}^{ideal} = \frac{P_i}{P_j} \quad (2)$$

And mixture gas separation factor α_{ij} was defined as the quotient of molar ratios of components in the permeate y_i and y_j divided by the quotient of molar ratio of components in the retentate x_i and x_j as in the following equation⁵⁰:

$$\alpha_{ij} = \frac{y_i/y_j}{x_i/x_j} \quad (3)$$

RESULTS AND DISCUSSION

Characterizations of MIL-68(Al) Crystals and MIL-68(Al)/Matrimid MMMs

Figure 2 shows the XRD patterns of the Matrimid, MIL-68(Al) crystals and MIL-68(Al)/Matrimid MMMs. The XRD pattern of MIL-68(Al) crystals [Figure 2(b)] displays all the typical peaks of MIL-68(Al), with the highest peak at $2\theta = 9.4^\circ$. This XRD pattern is in good agreement with literatures,^{43,45} thus confirming the formation of pure MIL-68(Al) crystal in this study. For MIL-68(Al)/Matrimid MMMs, the XRD pattern [Figure 2(c)] shows both the intense reflection peaks of MIL-68(Al) and the broad amorphous peak of Matrimid in Figure 2(a), suggesting that the membrane preparation procedure did not alter the crystal structure of MIL-68(Al).

Figure 3(a) shows the morphology of MIL-68(Al) crystals. It reveals that the MIL-68(Al) crystals display a typical needle-like morphology with size of ca. 400 nm in length and 100 nm in diameter. Similar morphologies are found in previous reports of

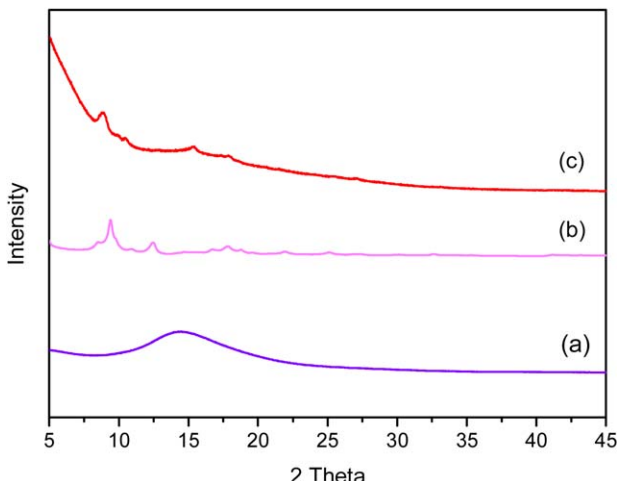


Figure 2. XRD patterns of the (a) as-synthesized Matrimid, (b) MIL-68(Al) crystals, and (c) MIL-68(Al)/Matrimid MMM. [Color figure can be viewed in the online issue, which is available at wileyonlinelibrary.com.]

MIL-68(Ga) and MIL-68(In), which are isostructures of MIL-68(Al), indicating the consistency of crystals morphology in this MOF group.⁵¹ For MIL-68(Al)/Matrimid MMM, both the top [Figure 3(b)] and cross-section FESEM [Figure 3(c,d)] show a homogeneous distribution of the MIL-68(Al) crystals in the Matrimid matrix without visible defects, exhibiting a favorable

interaction between the two phases. In particular, from the cross-section views, it can be seen that circular cavities and polymer veins (elongated matrix segments) are formed, which are evidences of this favorable interaction between the two phases. Perez *et al.* pointed out that circular cavities and polymer veins were indications of strong contact or interaction between the matrix and the filler crystals.⁴⁶ There are also some agglomerates of MIL-68(Al) crystals in the membrane, but no de-bonding of the agglomerates from the matrix is observed. It suggests that the interaction between the two phases were not strong enough to break the agglomerates and make them disperse at initial particle level, which is normal for nanoscale fillers in mixed matrix membranes.⁴⁶

Gas Permeation Tests of the MIL-68(Al)/Matrimid MMMs

Single Gas Permeation and Mixture Gas Separation. Table II shows the single gas permeability and the ideal separation factor of the CO₂ and CH₄ through the MIL-68(Al)/Matrimid MMMs at 373 K under the operation pressure of 1 and 4 bar. It can be seen that the CO₂ permeability (279.6 Barrer) is much higher than the CH₄ permeability (3.4 Barrer) at 373 K and 1 bar, with an ideal separation factor of 82.2, which by far exceeds the corresponding Knudsen coefficient of 0.6, suggesting that the MIL-68(Al)/Matrimid MMMs show a high separation performance for CO₂/CH₄ separation. Comparing with the CO₂ permeability of the pure polyimide membranes (about 126.9 Barrer in

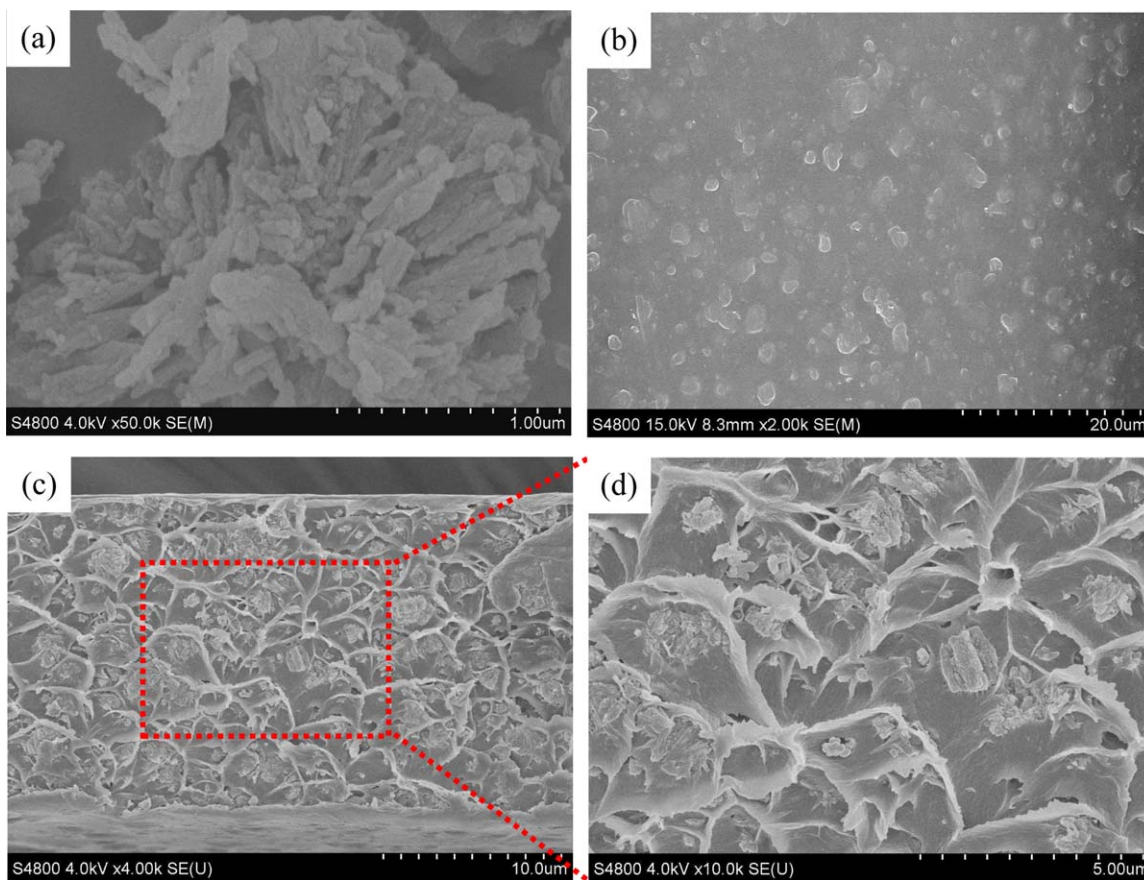


Figure 3. FESEM images of the (a) as-synthesized MIL-68(Al) crystals, (b) top and (c,d) cross-section views with different magnifications of the MIL-68(Al)/Matrimid MMM. [Color figure can be viewed in the online issue, which is available at wileyonlinelibrary.com.]

Table I. CO₂ Permeability and CO₂/CH₄ Selectivity of Different Membranes

Category	Membranes	Testing condition	P(CO ₂) Barrer ^a	α (CO ₂ /CH ₄)	Ref.
Polymer membranes	DDA-polyimide	303 K, 1 bar	200	26.3	56
	MDA-polyimide	303 K, 1 bar	110	27.5	56
	DATRI-polyimide	308 K, 1 bar	189	30.5	55
	Matrimid	308 K, 2 bar	8.4	39.4 ^a	35
MOF membranes	ZIF-90	498 K, 1 bar	1130 ^a	4.7	27
	ZIF-8	295 K, 1 bar	454,708 ^a	7.0	1
MMMs	MIL-53/polyimide-1	308 K, 1 bar	20.89	44.44	50
	MIL-53/polyimide-2	308 K, 1 bar	14.52	72.70	50
	MIL-53/Polyimide-3	308 K, 1 bar	14.69	76.88	50
	MIL-53/matrimid	308 K, 2 bar	40.0	90.1 ^c	35
	MIL-68 (Al)/PSF	308 K, 3 bar	4.7 ^c	36.5	45
	NH ₂ -MIL-125(Ti)/PSF	303 K, 3 bar	29.3 ^b	29.5	42
	ZIF-90A/polyimide	298K, 2 bar	720	37	57
	ZIF-90B/polyimide	298K, 2 bar	590	34	57
	MIL-68(Al)/polyimide	373 K, 1 bar	279.6	79.0	This work

Single gas permeability, except for ZIF-90A/PI, ZIF-90B/PI and ZIF-8, which are taken from mixed gas data.

^aData were calculated from the corresponding reported MOF membranes.

^bMixture gas permeability.

^cIdeal separation factor.

average in Table I), the CO₂ permeability of the MIL-68(Al)/Matrimid MMMs increases as much as 120%, while the CH₄ permeabilities for both pure polyimide membranes and MIL-68(Al)/Matrimid MMMs are almost the same, resulting in a great enhancement in the selectivity of CO₂/CH₄. Both CO₂ permeation and ideal separation factor of CO₂/CH₄ decrease when the operation pressure increases to 4 bar, which is normal phenomenon in MMMs.⁴² The influence of operation pressure on the separation performances of the MMM will be discussed in the following section.

The molecular sieve performances of the MIL-68(Al)/Matrimid MMMs were confirmed by the separation of equimolar CO₂/CH₄ mixture. Compared with the single gas permeability at 373 K and 1 bar, the CO₂ permeability (about 284.3 Barrer) in the mixture is quite stable, while the CH₄ permeability (about 3.6 Barrer) shows a slight increase, resulting in a slight decrease in CO₂/CH₄ selectivity (79.0), which also by far exceeds the corresponding Knudsen coefficient (Table II). The gas permeation in mixture is usually less than single gas permeation because of

competition between gas components.⁴⁷ Compared with other MMMs, these results indicate that the MIL-68(Al)/Matrimid MMM turns out to be one of the best MMMs in CO₂/CH₄ separation (Table I), which is in good agreement with a prediction from a molecular simulation study of MIL-68(Al).⁴³

Attributed to the addition of fillers which would facilitate the permeation of smaller gases, MMMs show high permselectivity or enhanced permeability with little reduction of selectivity, as reported in FAU-EMT/polyimide, MOF-199/polyimide, zeolite-4A/PVAc.^{39,52,53} Normally, for glassy polymers, diffusivity-selectivity is dominant in gas permeation because of the low mobility of glassy polymer chains, which is in favor of a faster permeation of smaller gases (e.g., CO₂) than larger ones (e.g., CH₄).⁵⁴ However, the gas permeation is always limited by the nature of the polymer. Therefore, in this work, we introduced MIL-68(Al) into Matrimid to prepare high permselectivity MIL-68(Al)/Matrimid MMMs. On the one hand, the introduction of MIL-68(Al) nanocrystals will increase the free volume of the Matrimid which will facilitate the gas permeation, and thus the

Table II. CO₂/CH₄ Separation Performances for MIL-68(Al)/Matrimid Mixed Matrix Membranes under Different Operation Pressures

Operation pressure	Knudsen coefficient	Separation performances of the MIL-68(Al)/Matrimid MMM					
		Single gas			Mixed gases		
		Permeability (CO ₂) (Barrer)	Permeability (CH ₄) (Barrer)	Ideal separation factor	Permeability (CO ₂) (Barrer)	Permeability (CH ₄) (Barrer)	Separation factor
1 bar	0.6	279.6	3.4	82.2	284.3	3.6	79.0
4 bar		176.6	3.2	55.2	164.5	3.1	53.1

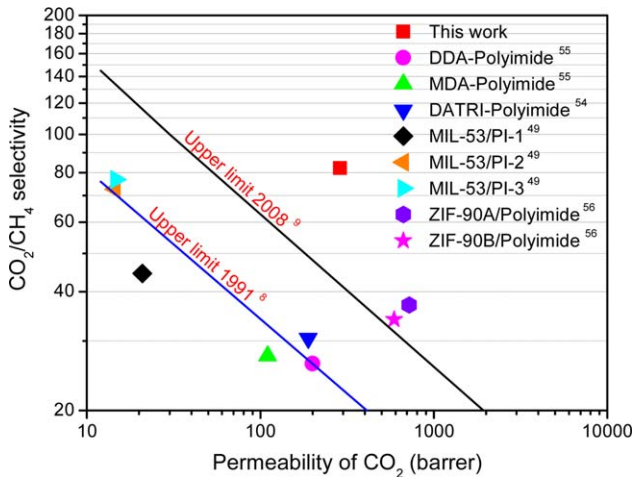


Figure 4. CO₂/CH₄ mixture selectivity versus CO₂ permeability of the MIL-68(Al)/Matrimid MMM compared with those of polyimide membranes and mixed matrix membranes. The upper bound trade-off lines are those summarized by Robeson in 1991,⁸ and 2008.⁹ [Color figure can be viewed in the online issue, which is available at wileyonlinelibrary.com.]

gas transport in the MIL-68(Al)/Matrimid MMMs is dominated by solubility-selectivity rather than diffusivity-selectivity.¹⁴ Therefore, more condensable gases (e.g., CO₂) are more permeable than less condensable gases (e.g., CH₄).⁶ On the other hand, MIL-68(Al), with large pores (6.0–6.4, 16–17 Å) and abundant hydroxyl groups along the channel direction, shows high adsorption affinity to CO₂, resulting in significant increase of CO₂ permeability. These synergetic effects of solubility, absorbability, and diffusivity lead to the favorable permeation of CO₂ and excellent separation performance of CO₂/CH₄.

The CO₂ permeability and CO₂/CH₄ selectivity of the as-prepared MIL-68(Al)/Matrimid MMMs are drawn in the Robeson upper bound plot, as shown in Figure 4. For comparison, the permselectivities of polyimide membranes and MMMs are also shown in Figure 4 and Table I. It can be seen that the permselectivity of the MIL-68(Al)/Matrimid MMMs is much higher than other MMMs and polyimide membranes, and also far exceeds the Robeson upper bound.^{9,55–57} These results highly recommend that the MIL-68(Al)/Matrimid MMM is a promising material for the separation of CO₂ in natural gas industry.

Effect of Operation Pressure on the Separation Performances. To get a profound view of the effect of operation pressure on the permselectivity of the MIL-68(Al)/Matrimid MMMs, the MIL-68(Al)/Matrimid MMMs were tested with the separation of CO₂/CH₄ with operation pressure ranging from 1 to 5 bar. Figure 5 shows the gas permeability and CO₂/CH₄ selectivity of the MIL-68(Al)/Matrimid MMMs as a function of operation pressure at 373 K. It can be seen that with increasing pressure, the CO₂ permeability decreases, while CH₄ permeability remains almost constant, leading to a decrease of CO₂/CH₄ selectivity. Similar phenomena are usually observed for other MMMs.^{39,58} Different from the diffusion-dependent permeation, the permeation in this study is controlled by solution and adsorption mode.¹⁴ As mentioned above, MIL-68(Al) shows a

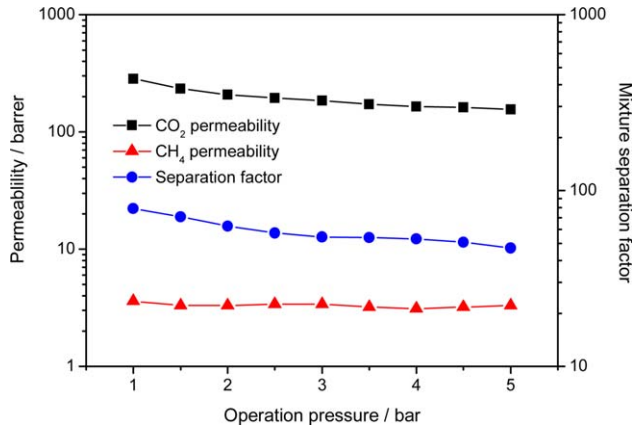


Figure 5. The permeability of CO₂ and CH₄ as well as CO₂/CH₄ mixture separation factor of the MIL-68(Al)/Matrimid MMM for the separation of an equimolar CO₂/CH₄ mixture as a function of operation pressure at 373 K. [Color figure can be viewed in the online issue, which is available at wileyonlinelibrary.com.]

high adsorption affinity and capacity of CO₂ over CH₄.⁴³ With increasing permeation pressure, the adsorption affinity of CO₂ decreases, thus resulting in a decrease of CO₂ permeability and CO₂/CH₄ selectivity. Further, the results indicate that CO₂ shows higher solubility in Matrimid polymer and higher adsorbility in the MIL-68(Al) pores than CH₄.^{6,43} As pressure increases, the CO₂ molecules dissolved in the matrix and adsorbed at the MIL-68(Al) sorption sides become saturated and keep unchanged until the penetrants plasticizes the polymer at the plasticization pressure. Diestel *et al.* found that the CO₂ permeability kept decreasing until reaching a minimum at the plasticization pressure under which permeability increased again.⁶ A phenomenon to be noted is that with increasing pressure, the flux still increases. However, after corrected by pressure, the permeability shows a decreasing trend. In a word, the increased amount of gases is not proportionate to the increase

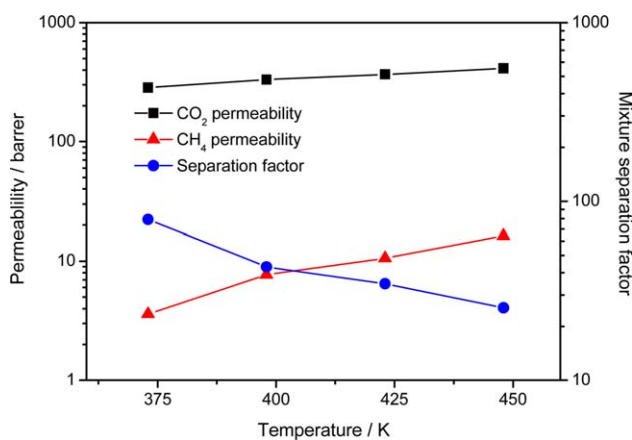


Figure 6. The permeability of CO₂ and CH₄ as well as CO₂/CH₄ mixture separation factor of the MIL-68(Al)/Matrimid MMM for the separation of an equimolar CO₂/CH₄ mixture as a function of operation temperature under 1 bar. [Color figure can be viewed in the online issue, which is available at wileyonlinelibrary.com.]

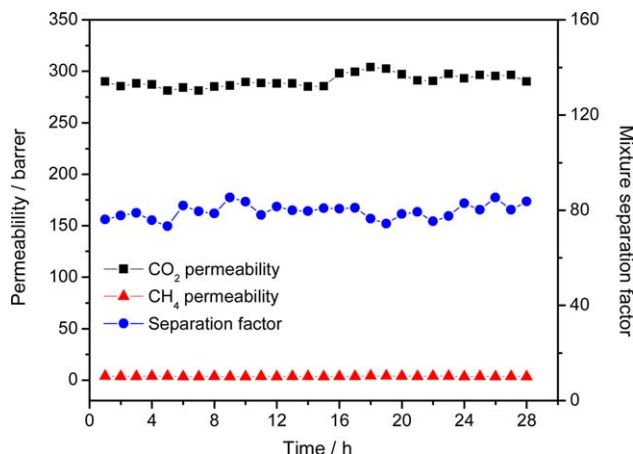


Figure 7. Stability measurement of the MIL-68(Al)/Matrimid MMM for the separation of an equimolar CO₂/CH₄ mixture at 373 K and 1 bar. [Color figure can be viewed in the online issue, which is available at wileyonlinelibrary.com.]

of pressure. Similar phenomenon was also observed by Rodenas *et al.*⁴⁰

Effect of Operation Temperature on the Separation Performances. Temperature is an important factor in determining the separation performances of MMMs. Therefore, we tested the effect of operation temperature on the permselectivity of the MIL-68(Al)/Matrimid MMMs at 1 bar. Figure 6 shows the gas permeability and CO₂/CH₄ selectivity of the MIL-68(Al)/Matrimid MMMs as a function of operation temperature. As shown in Figure 6, both CO₂ and CH₄ permeabilities increase with increasing temperature, but CH₄ permeability increases more obviously, thus resulting in a decrease of CO₂/CH₄. Similar phenomenon is seen in the work of Chen *et al.*⁴⁹ The diffusion of gases relates with the amount of energy required by the penetrants to execute a diffusive jump through the membrane, and with increasing temperature, the energy provided for diffusive jumping increases. Therefore, under a temperature range without significant thermal transitions of the polymer matrix, the diffusion coefficient typically increases considerably with increasing temperature.⁴⁹ Larger molecules such as CH₄ will execute more jumps at high temperature because they have more limited opportunities at low temperature.⁴⁹ Further, in this work, since CH₄ molecules have relatively weak interaction with the MIL-68(Al) crystals and Matrimid matrix, permeation of CH₄ through the motivated polymer chains increases more than CO₂ at high temperatures, thus leading to a decrease in the CO₂/CH₄ selectivity. Further, the MIL-68(Al)/Matrimid MMMs have been tested for more than 24 h for the separation of equimolar CO₂/CH₄ mixtures at 373 K and 1 bar. It can be seen that both the CO₂/CH₄ selectivity and the CO₂ permeability remained unchanged (Figure 7), suggesting that the MIL-68(Al)/Matrimid MMMs show a high stability in the CO₂/CH₄ separation.

CONCLUSIONS

In conclusion, we have successfully synthesized a novel MIL-68(Al)/Matrimid MMM for the separation of CO₂/CH₄ mixture.

It is found that the MIL-68(Al)/Matrimid MMMs show high permselectivity for CO₂/CH₄ separation. At 373 K and 1 bar, the CO₂ permeability and the CO₂/CH₄ selectivity are 284.3 Barrer and 79.0, respectively, which are much higher than the Robeson upper bound limit and those of previously reported MMMs. Both the operation pressure and temperature have a significant effect on the separation performance of the MIL-68(Al)/Matrimid MMM. Further, the MIL-68(Al)/Matrimid MMM shows a high stability in the long-term separation of CO₂/CH₄ at 373 K and 1 bar. These properties recommend the developed MIL-68(Al)/Matrimid MMM as a promising candidate for the purification of natural gases. Future work will focus on different loadings and their permselectivity.

ACKNOWLEDGMENTS

Financial support by the Chinese Academy of Science Visiting Professorship for Senior International Scientists (Grant No. 2013T1G0047), External Cooperation Program of BIC, Chinese Academy of Science (Grant No. 174433KYSB2013005), and Ningbo Science and Technology Innovation Team (Grant No. 2014B81004) is acknowledged.

REFERENCES

- Venna, S. R.; Carreon, M. A. *J. Am. Chem. Soc.* **2010**, *132*, 76.
- Carreon, M. A.; Li, S.; Falconer, J. L.; Noble, R. D. *J. Am. Chem. Soc.* **2008**, *130*, 5412.
- Xiao, Y.; Low, B. T.; Hosseini, S. S.; Chung, T. S.; Paul, D. R. *Prog. Polym. Sci.* **2009**, *34*, 561.
- Moradihamedani, P.; Ibrahim, N. A.; Yunus, W. M. Z. W.; Yusof, N. A. *J. Appl. Polym. Sci.* **2013**, *130*, 1139.
- Zhang, Y.; Sunarso, J.; Liu, S.; Wang, R. *Int. J. Greenh. Gas Con.* **2013**, *12*, 84.
- Diestel, L.; Wang, N.; Schulz, A.; Steinbach, F.; Caro, J. *Ind. Eng. Chem. Res.* **2015**, *54*, 1103.
- Sridhar, S.; Smitha, B.; Aminabhavi, T. M. *Sep. Purif. Rev.* **2007**, *36*, 113.
- Robeson, L. M. *J. Membr. Sci.* **1991**, *62*, 165.
- Robeson, L. M. *J. Membr. Sci.* **2008**, *320*, 390.
- Japip, S.; Wang, H.; Xiao, Y.; Shung Chung, T. *J. Membr. Sci.* **2014**, *467*, 162.
- Liu, X.; Hu, D.; Li, M.; Zhang, J.; Zhu, Z.; Zeng, G.; Zhang, Y.; Sun, Y. *J. Appl. Polym. Sci.* **2015**, *132*.
- Powell, C. E.; Duthie, X. J.; Kentish, S. E.; Qiao, G. G.; Stevens, G. W. *J. Membr. Sci.* **2007**, *291*, 199.
- Yong, W. F.; Li, F. Y.; Xiao, Y. C.; Li, P.; Pramoda, K. P.; Tong, Y. W.; Chung, T. S. *J. Membr. Sci.* **2012**, *407-408*, 47.
- Chung, T. S.; Jiang, L. Y.; Li, Y.; Kulprathipanja, S. *Prog. Polym. Sci.* **2007**, *32*, 483.
- Mahajan, R.; Koros, W. *J. Ind. Eng. Chem. Res.* **2000**, *39*, 2692.
- Won, J. G.; Seo, J. S.; Kim, J. H.; Kim, H. S.; Kang, Y. S.; Kim, S. J.; Kim, Y. M.; Jegal, J. G. *Adv. Mater.* **2005**, *17*, 80.

17. Xiao, Y. L.; Guo, X. Y.; Huang, H. L.; Yang, Q. Y.; Huang, A. S.; Zhong, C. L. *RSC Adv.* **2015**, *5*, 7253.
18. Farrukh, S.; Minhas, F. T.; Hussain, A.; Memon, S.; Bhanger, M. I.; Mujahid, M. *J. Appl. Polym. Sci.* **2014**, *131*,
19. Rezakazemi, M.; Shahidi, K.; Mohammadi, T. *Int. J. Hydrogen Energ.* **2012**, *37*, 14576.
20. Zornoza, B.; Seoane, B.; Zamaro, J. M.; Tellez, C.; Coronas, J. *ChemPhysChem* **2011**, *12*, 2781.
21. Valero, M.; Zornoza, B.; Tellez, C.; Coronas, J. *Microporous Mesoporous Mater.* **2014**, *192*, 23.
22. Khan, M. M.; Filiz, V.; Bengtson, G.; Shishatskiy, S.; Rahman, M. M.; Lillepaerg, J.; Abetz, V. *J. Membr. Sci.* **2013**, *436*, 109.
23. Wu, H.; Li, X. Q.; Li, Y. F.; Wang, S. F.; Guo, R. L.; Jiang, Z. Y.; Wu, C.; Xin, Q. P.; Lu, X. *J. Membr. Sci.* **2014**, *465*, 78.
24. Vatanpour, V.; Madaeni, S. S.; Rajabi, L.; Zinadini, S.; Derakhshan, A. A. *J. Membr. Sci.* **2012**, *401*, 132.
25. Duan, C.; Kang, G.; Liu, D.; Wang, L.; Jiang, C.; Cao, Y.; Yuan, Q. *J. Appl. Polym. Sci.* **2014**, *131*,
26. Kanehashi, S.; Gu, H.; Shindo, R.; Sato, S.; Miyakoshi, T.; Nagai, K. *J. Appl. Polym. Sci.* **2013**, *128*, 3814.
27. Xie, L.; Liu, D.; Huang, H.; Yang, Q.; Zhong, C. *Chem. Eng. J.* **2014**, *246*, 142.
28. Shah, M.; McCarthy, M. C.; Sachdeva, S.; Lee, A. K.; Jeong, H. K. *Ind. Eng. Chem. Res.* **2012**, *51*, 2179.
29. Rosi, N. L.; Eckert, J.; Eddaoudi, M.; Vodak, D. T.; Kim, J.; O'Keeffe, M.; Yaghi, O. M. *Science* **2003**, *300*, 1127.
30. Lee, J.; Farha, O. K.; Roberts, J.; Scheidt, K. A.; Nguyen, S. T.; Hupp, J. T. *Chem. Soc. Rev.* **2009**, *38*, 1450.
31. Volkinger, C.; Loiseau, T.; Férey, G.; Morais, C. M.; Taulelle, F.; Montouillout, V.; Massiot, D. *Microporous Mesoporous Mater.* **2007**, *105*, 111.
32. Yamada, T.; Kitagawa, H. *J. Am. Chem. Soc.* **2009**, *131*, 6312.
33. Millward, A. R.; Yaghi, O. M. *J. Am. Chem. Soc.* **2005**, *127*, 17998.
34. Song, Q.; Nataraj, S. K.; Roussenova, M. V.; Tan, J. C.; Hughes, D. J.; Li, W.; Bourgoin, P.; Alam, M. A.; Cheetham, A. K.; Al-Muhtaseb, S. A.; Sivaniah, E. *Energ. Environ. Sci.* **2012**, *5*, 8359.
35. Hsieh, J. O.; Balkus, K. J.; Ferraris, J. P.; Musselman, I. H. *Microporous Mesoporous Mater.* **2014**, *196*, 165.
36. Thompson, J. A.; Chapman, K. W.; Koros, W. J.; Jones, C. W.; Nair, S. *Microporous Mesoporous Mater.* **2012**, *158*, 292.
37. Kanehashi, S.; Chen, G. Q.; Scholes, C. A.; Ozcelik, B.; Hua, C.; Ciddor, L.; Southon, P. D.; D'Alessandro, D. M.; Kentish, S. E. *J. Membr. Sci.* **2015**, *482*, 49.
38. Moradihamedani, P.; Ibrahim, N. A.; Ramimoghadam, D.; Yunus, W. M. Z. W.; Yusof, N. A. *J. Appl. Polym. Sci.* **2014**, *131*,
39. Nik, O. G.; Chen, X. Y.; Kaliaguine, S. *J. Membr. Sci.* **2012**, *413*, 48.
40. Rodenas, T.; van Dalen, M.; Serra-Crespo, P.; Kapteijn, F.; Gascon, J. *Microporous Mesoporous Mater.* **2014**, *192*, 35.
41. Amooghin, A. E.; Omidkhah, M.; Kargari, A. *RSC Adv.* **2015**, *5*, 8552.
42. Guo, X. Y.; Huang, H. L.; Ban, Y. J.; Yang, Q. Y.; Xiao, Y. L.; Li, Y. S.; Yang, W. S.; Zhong, C. L. *J. Membr. Sci.* **2015**, *478*, 130.
43. Yang, Q.; Vaesen, S.; Vishnuvarthan, M.; Ragon, F.; Serre, C.; Vimont, A.; Daturi, M.; De Weireld, G.; Maurin, G. *J. Mater. Chem.* **2012**, *22*, 10210.
44. Junaidi, M. U. M.; Leo, C. P.; Kamal, S. N. M.; Ahmad, A. L.; Chew, T. L. *Fuel Process. Technol.* **2013**, *112*, 1.
45. Seoane, B.; Sebastián, V.; Tellez, C.; Coronas, J. *CrystEngComm.* **2013**, *15*, 9483.
46. Perez, E. V.; Balkus, K. J.; Ferraris, J. P.; Musselman, I. H. *J. Membr. Sci.* **2009**, *328*, 165.
47. Huang, A. S.; Dou, W.; Caro, J. *J. Am. Chem. Soc.* **2010**, *132*, 15562.
48. Liu, Q.; Wang, N.; Caro, J.; Huang, A. *J. Am. Chem. Soc.* **2013**, *135*, 17679.
49. Chen, X. Y.; Vinh-Thang, H.; Rodrigue, D.; Kaliaguine, S. *RSC Adv.* **2013**, *3*, 24266.
50. Chen, X. Y.; Vinh-Thang, H.; Rodrigue, D.; Kaliaguine, S. *Ind. Eng. Chem. Res.* **2012**, *51*, 6895.
51. Volkinger, C.; Meddouri, M.; Loiseau, T.; Guillou, N.; Marrot, J.; Ferey, G.; Haouas, M.; Taulelle, F.; Audebrand, N.; Latroche, M. *Inorg. Chem.* **2008**, *47*, 11892.
52. Nik, O. G.; Chen, X. Y.; Kaliaguine, S. *J. Membr. Sci.* **2011**, *379*, 468.
53. Adams, R. T.; Lee, J. S.; Bae, T. H.; Ward, J. K.; Johnson, J. R.; Jones, C. W.; Nair, S.; Koros, W. J. *J. Membr. Sci.* **2011**, *367*, 197.
54. Du, N.; Park, H. B.; Dal-Cin, M. M.; Guiver, M. D. *Energy Environ. Sci.* **2012**, *5*, 7306.
55. Cho, Y. J.; Park, H. B. *Macromol. Rapid Commun.* **2011**, *32*, 579.
56. Al-Masri, M.; Fritsch, D.; Kricheldorf, H. R. *Macromolecules* **2000**, *33*, 7127.
57. Bae, T. H.; Lee, J. S.; Qiu, W.; Koros, W. J.; Jones, C. W.; Nair, S. *Angew. Chem. Int. Ed.* **2010**, *49*, 9863.
58. Shahid, S.; Nijmeijer, K. *J. Membr. Sci.* **2014**, *459*, 33.